ChemBioChem

Research Article
doi.org/10.1002/cbic.202100582

Chemistry
Europe
European Chemical
Societies Publishing

www.chembiochem.org

Monitoring the Response of Multiple Signal Network Components to Acute Chemo-Optogenetic Perturbations in Living Cells

Manuela Kowalczyk+,[a] Dominic Kamps+,[b] Yaowen Wu,[c] Leif Dehmelt,*[b] and Perihan Nalbant*[a]

Cells process information via signal networks that typically involve multiple components which are interconnected by feedback loops. The combination of acute optogenetic perturbations and microscopy-based fluorescent response readouts enables the direct investigation of causal links in such networks. However, due to overlaps in spectra of photosensitive and fluorescent proteins, current approaches that combine these methods are limited. Here, we present an improved chemo-optogenetic approach that is based on switch-like perturbations induced by a single, local pulse of UV light. We show that this approach can be combined with parallel monitoring of multiple fluorescent readouts to directly uncover relations between signal network components. We present the application of this technique to directly investigate feedback-controlled regulation in the cell contraction signal network that includes GEF-H1, Rho and Myosin, and functional interactions of this network with tumor relevant RhoA G17 mutants.

Introduction

Many cellular functions require dynamic cell shape changes. For example, migrating cells generate segregated subcellular domains that drive cell protrusion and cell contraction. Furthermore, in critical steps during embryonic development, cells generate local contractile pulses that drive multi-cellular rearrangements.[1] These dynamic processes are coordinated in space and time by signal networks with multiple components that are interconnected by feedback regulation. Investigations of such signal networks are challenging because causal relationships are ambiguous, as interlinked components in feedback loops act both downstream and upstream of one another.[2] To

investigate such signal networks, measurements of dynamic responses to acute perturbations are very valuable.

Optogenetic tools enable rapid, light-induced triggering of such acute perturbations. However, combining fluorescent readouts with standard optogenetic techniques is limited due to the overlap between their activation spectra and typical wavelengths used for fluorescence excitation. To overcome these limitations, we recently developed a generic photo-chemical dimerization approach that we termed molecular activity painting.[3]

This perturbation approach is triggered by irreversible photo-uncaging with a single UV light pulse, and it enables acute targeting of signal molecules to the plasma membrane with μm precision.[3,4] The perturbation follows simple pseudo-first order association kinetics, which facilitates a clean interpretation of dynamic fluorescent response readouts. This allowed investigations of signal processing in the GEF-H1, Rho, Myosin cell contraction signal network by fitting the observed perturbation and response kinetics to simulations of network dynamics.[4] However, these established implementations only allowed the simultaneous readout of the response of one signal network component and were therefore limited in their application to directly investigate, how multiple interconnected signal network components influence each other in response to an acute perturbation.

Here, we extended the molecular activity painting approach to enable parallel readout of the perturbation kinetics together with the response kinetics of two distinct signal network components. We applied this approach to investigate relations between multiple interconnected components in Rho GTPase signal networks: a) The feedback-controlled interplay between the GTPase Rho and its effector Myosin-IIa after acute perturbation with the Rho activator GEF-H1 and b) the interactions of the tumor related Rho G17E and G17V mutants

[a] Dr. M. Kowalczyk,+ Prof. P. Nalbant
Department of Molecular Cell Biology
Center for Medical Biotechnology
University of Duisburg-Essen, 45141 Essen (Germany)
E-mail: perihan.nalbant@uni-due.de

[b] D. Kamps,+ L. Dehmelt
Department of Chemistry and
Chemical Biology and Department of Systemic Cell Biology
TU Dortmund University and
Max-Planck-Institute of Molecular Physiology
44227 Dortmund (Germany)
E-mail: Leif.Dehmelt@tu-dortmund.de

[c] Prof. Y. Wu
Department of Chemistry
Umeå Centre for Microbial Research
Umeå University, 901 87 Umeå (Sweden)

[+] These authors contributed equally to this work.

ChemBioChem

Research Article
doi.org/10.1002/cbic.202100582

Chemistry
Europe
European Chemical
Societies Publishing

with these signal network components. With these two examples we demonstrate the general applicability of this method to investigate causal links between signal network components in their natural, cellular environment, and to study the molecular mechanisms, by which such signal networks are perturbed during cancer progression.

Results and Discussion

The original molecular activity painting approach is based on light-based triggering of a rapid and irreversible increase in the local concentration of a protein of interest at the plasma membrane.[3] The technique is particularly tailored to cell biological questions that are related to signals at or near the plasma membrane, such as growth factor receptor signaling or regulators of cytoskeletal dynamics. Rapid plasma membrane targeting is triggered by uncaging of a photodimerizer, that is covalently bound to an artificial receptor. Diffusion of the uncaged photodimerizer is prevented by an interaction between antigen epitopes at the extracellular domain of the artificial receptor with surface-immobilized antibodies. The original antibody surface immobilization protocol, that was based on DNA-directed immobilization, was subsequently simplified by using surface-adsorbed biotinylated Poly-L-lysine as a linking agent.[4] The method is limited to perturbations that can be introduced by increasing the local concentration at the plasma membrane, and due to the irreversible nature of the approach, control of the perturbation dynamics is limited. However, as the method only requires a single pulse of light, technical challenges related to local, continuous illumination or phototoxicity are alleviated.

The original molecular activity painting system consists of three components, each of which was labeled with a distinct fluorescent protein suitable for prolonged live cell imaging: mCitrine on the artificial receptor, mTurquoise2 on the protein used to induce the perturbation, and mCherry on the response read-out protein. However, to use molecular activity painting, it is sufficient to monitor the perturbation and response proteins, but it is not necessary to detect the artificial receptor. We therefore reasoned that mCitrine could be used to monitor a second response read-out in a system with unlabeled or blue fluorescent protein tagged artificial receptors (Figure 1A). Unfortunately, artificial receptors that simply lack a fluorescent protein or that contain the common monomeric blue fluorescent protein (mTagBFP2) were not efficiently expressed at the plasma membrane and accumulated in internal cellular structures, presumably due to inefficient folding or inefficient processing through the secretory pathway. Consequently, these receptors performed very poorly, as their proper localization is critical for efficient plasma membrane targeting. The fluorescent protein moxBFP was developed for optimal folding[5] and could thereby facilitate the processing and plasma membrane targeting of artificial receptors. Flanking of protein domains by a short coiled-coil linker motif can provide additional stability in fusion proteins. Indeed, artificial receptors that are labeled with coiled-coil flanked moxBFP were efficiently expressed at the plasma
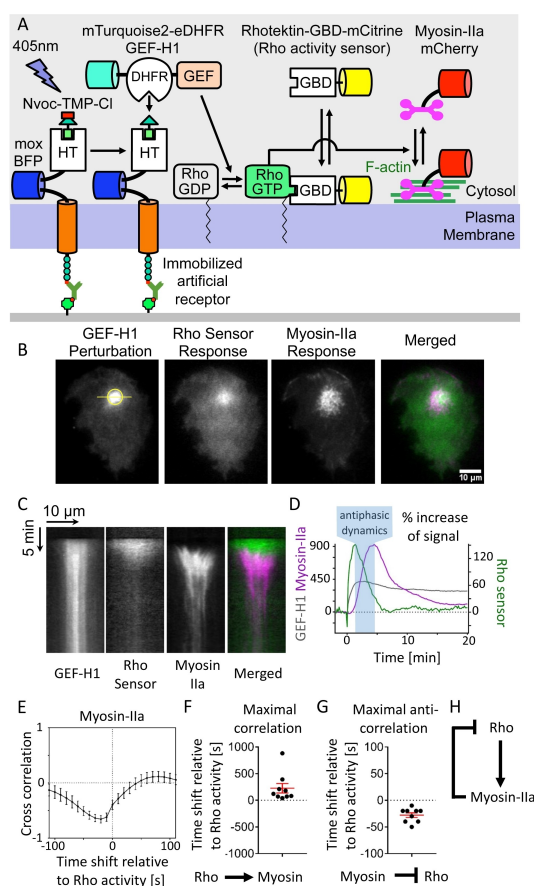

Figure 1. Direct investigation of signal processing in cell contraction regulation via acute GEF-H1 perturbation and parallel Rho activity and Myosin response readouts. (A) Schematic representation of an improved variant of molecular activity painting that enables parallel readout of two response kinetics following an acute signal network perturbation. Light induced uncaging of a NvocTMP-Cl photo-dimerizer covalently linked to the HaloTag (HT) on immobilized artificial receptors, leads to plasma membrane targeting of an eDHFR fusion protein. Here, these components were co-expressed in U2OS cells to investigate cell contraction regulation: Light-induced plasma membrane targeting of the RhoGEF GEF-H1 activates the small GTPase Rho and recruits the downstream effector Myosin-IIa. The change in Rho activity is detected by measuring the plasma membrane translocation of the GTPase-binding domain (GBD) of Rhotekin. (B–D) TIRF-microscopy based analysis of the Rho activity and Myosin-IIa response dynamics in a representative U2OS cell after acute GEF-H1 perturbation. Color merged images in (B) and (C) show the Rho activity sensor (green) and Myosin-IIa (magenta). (B) TIRF images of the stable GEF-H1 perturbation and Rho activity sensor and Myosin-IIa plasma membrane recruitment response 3 minutes after illumination (See also Supporting Information Movie 1). (C) Kymographs corresponding to the yellow line shown in (B). (D) Perturbation and response kinetics measured in the yellow circle in (B). The increase of the fluorescent signal in percent above initial values is shown. (E–G) Temporal cross-correlation analysis of Myosin-IIa and Rho activity after GEF-H1 perturbation (n = 9 cells from three independent experiments). (E) Cross-correlation function of Myosin-IIa and Rho activity sensor signal (mean with SEM). (F–G) Time shifts with maximal correlation (F) or maximal anti-correlation (G) between the Myosin-IIa and the Rho activity sensor responses obtained from individual cells (mean with SEM). It should be noted that the maximum (+70s) and minimum (-20s) in the average cross-correlation function for all cells (E) are not necessarily the same as the corresponding average of values obtained on the single cell level (F: +227 +/-89 s and G: −28 +/-4 s). (H) Schematic of a proposed negative feedback loop between Rho and Myosin that was derived from the interpretation of correlated response dynamics indicated in bottom panels of (F–G).

membrane and their performance was indistinguishable from mCitrine-labeled receptors (Figure S1).

Next, we used this approach to study the perturbation-response dynamics of a signal network that controls cell contraction.[6] We introduced perturbations into this signal network by acute photochemical targeting of the Rho activator GEF-H1 to the plasma membrane. We combined this perturbation with the parallel readout of the activity state of endogenous Rho using the activity sensor that is based on the Rhotekin GTPase-binding domain (GBD) and plasma membrane recruitment of the Rho effector Myosin-IIa (Figure 1A). To avoid competition between the GBD and endogenous Rho effectors, we expressed this molecule at very low levels using a truncated promotor,[7] and we used a sensitive EMCCD camera to detect these small sensor amounts.

As both the perturbation and the two responses are based on the translocation of proteins from the cytosol to the plasma membrane, total internal reflection fluorescence microscopy (TIRF−M) was used to measure their kinetics in living cells. This enabled us to investigate the relationship between these three components in the cell contraction signal network. Interestingly, we found that the dynamics of these two components are antiphasic and overlap only minimally in space and time (Figure 1B–D, Figure S2 and Supporting Information Movie 1).

Our improved molecular activity painting method enables us to perform analysis in individual cells, and we were thus able to extract additional information about cell-to-cell variability. First, comparison of the overall strength of the two responses by measuring the area under the curves above background signals, showed that Myosin activity is dependent on the dose of Rho activity (Figure S3A). This observation is in agreement with the well-accepted idea that Myosin-IIa is activated by Rho effectors.[8] In addition, we performed cross-correlation analyses to investigate the relation between the temporal response profiles. These analyses revealed a weak positive correlation of Myosin-IIa plasma membrane targeting with a relatively long time shift of $227+/-89$ s after Rho activity (Figure 1E,F). This time shift shows that the activation of Myosin-IIa after Rho activation is a relatively slow process with a high cell-to-cell variability (Figure 1E,F). The single cell analyses also revealed a strong anti-correlation with a short time shift for Myosin-IIa plasma membrane targeting before Rho activity, which was less variable and much shorter with an average value of $28+/-4$ s (Figure 1E,G). This anti-correlation primarily reflects the anti-phasic activity dynamics of Rho and Myosin between the activity maxima of these components (Figure 1D). This shows that increased Myosin signal precedes a decrease in Rho activity, which supports the idea that Myosin-IIa can somehow inhibit Rho activity. This could for example be mediated by the inhibitory interaction between Myosin-IIa and the DH domain of GEF-H1.[9] Importantly, clear anti-correlation was observed in all cells (Figure S3B), showing that this effect is robust against cell-to-cell variability.

Together, the activation of Myosin by Rho and the inhibition of Rho by Myosin close a negative feedback loop, via which Rho can inhibit its own activity (Figure 1H). Interestingly, the single-cell analyses show that this inhibitory action is very rapid and

robust. Such a robust inhibitory action of Myosin-IIa on its upstream activator Rho might represent a safeguard mechanism that prevents unrestrained cell contraction, which might otherwise interfere with normal cell function.

Next, we investigated the molecular mode of action of Rho GTPases that carry tumor-associated mutations, in particular the RhoA G17E mutant.[10] Previous reports suggested that this mutant might have a dominant negative effect on Rho activity and might thereby inhibit a potential tumor suppressor function of wild-type Rho.[10a,11] However, the mechanism of this dominant negative effect was not well understood and direct evidence in living cells was lacking. Using the molecular activity painting method, we introduced perturbations by locally increasing the level of RhoA mutants, and simultaneously measured both the activity state of these mutants, using the Rho activity sensor and their interaction with the upstream activator GEF-H1 (Figure 2A). Using this approach, we found that acute, light-triggered plasma membrane targeting of RhoA
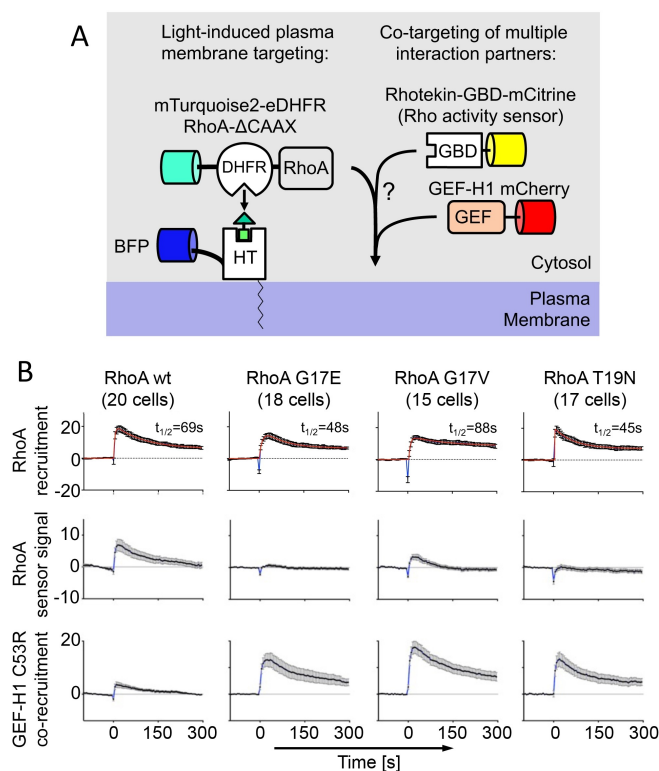

Figure 2. RhoA G17E is inactive and acts as a dominant negative mutant by sequestering GEF-H1. (A) Schematic representation of plasma membrane targeting of wild-type or mutant RhoA lacking its CAAX box membrane anchor (ΔCAAX) via light-induced uncaging of the NvocTMP−Cl photo-dimerizer. NvocTMP−Cl was located to the plasma membrane via the KRas CAAX box linked to HaloTag (HT). Co-recruitment of upstream GEF activator and the downstream effector GTPase-binding domain (GBD) was measured in parallel to the perturbation. (B) Co-recruitment kinetics in U2OS cells that express the constructs depicted in A. The increase of the fluorescent signal in percent above initial values is shown. Measurements were performed in small areas of the plasma membrane indicated by white circles in Figure S4A (n = 17–20 cells from 3–4 independent experiments. Error bars represent SEM). Blue lines connect individual measurements, red lines represent non-linear fits of the perturbation kinetics to obtain indicated decay half-times, which are primarily due to lateral diffusion of the uncaged dimerizer on CAAX box linked to HaloTag (see Supporting Information for details).

G17E does not co-recruit the Rho activity sensor, showing that this mutant is inactive. However, this mutant very efficiently co-recruited the Rho activator GEF-H1, showing that these proteins strongly interact with each other in living cells (Figure 2B and Figure S4B; Supporting Information Movie 2). This interaction could sequester GEF-H1 and prevent it from activating endogenous wild-type RhoA, and thereby explain the proposed dominant negative effect of RhoA G17E. Similar observations were made with the well-established dominant negative RhoA mutant T19 N.[12] This was in contrast to local RhoA wild-type (wt) perturbations, which triggered a robust local increase in Rho activity levels and only a modest increase in GEF-H1 (Supporting Information Movie 3). This modest increase is presumably due to the PH domain, which is known to bind active Rho.[4,13] Another tumor associated RhoA G17 variant, the G17V mutant, also co-recruited GEF-H1. However, this mutant still showed some residual effector binding indicating that it is not fully inactive.

Next, we investigated if the RhoA G17E mutant indeed acts dominant negative in cells and can inhibit the activation of endogenous Rho by endogenous GEF-H1. To test this, we capitalized on an assay that we established previously, in which we acutely released endogenous, sequestered GEF-H1 by depolymerizing microtubules with the pharmacological compound nocodazole.[6,14] This treatment increases local Rho activity dynamics via a signal network that includes a positive feedback between GEF-H1 and RhoA and a myosin-dependent negative feedback.[4,6] The increased local activity dynamics of endogenous Rho can be monitored in living cells using the Rho activity sensor.[6] Indeed, in cells that co-express the control plasmid (EGFP) or EGFP-fused wild-type Rho (Figure 3A–C), nocodazole treatment strongly stimulated local Rho activity. In contrast, co-expression of RhoA G17E (Figure 3A–C) completely inhibited GEF-H1 stimulated Rho activity dynamics. This shows that RhoA G17E strongly suppresses endogenous wild-type Rho activity dynamics downstream of GEF-H1. Furthermore, RhoA G17E also inhibited the formation of strong stress fibers downstream of nocodazole-stimulated GEF-H1 release (Figure 3D,E).

Therefore, RhoA G17E inhibits Rho activity dynamics in a dominant negative fashion by sequestering GEF-H1 to prevent amplification of wild-type Rho activity. Combined with the lack of effector interaction, this dominant negative function might interfere with the proposed tumor suppressive role of Rho wild-type and thereby promote tumor progression.[10a,11]

In conclusion, we present an improved version of molecular activity painting, which is easily implemented, and enables parallel readout of multiple response dynamics after acute, light-triggered perturbations in individual, living cells. We show that such parallel readouts enable direct investigations of precise temporal relations between interconnected signal network components. Due to cell-to-cell variability, such relations are not accessible with other methods that rely on averaging of dynamic measurements from multiple cells.

The presented acute perturbation and response analysis directly reveals a causal relationship between the GEF-H1 perturbation and the Rho and Myosin-IIa response, and the
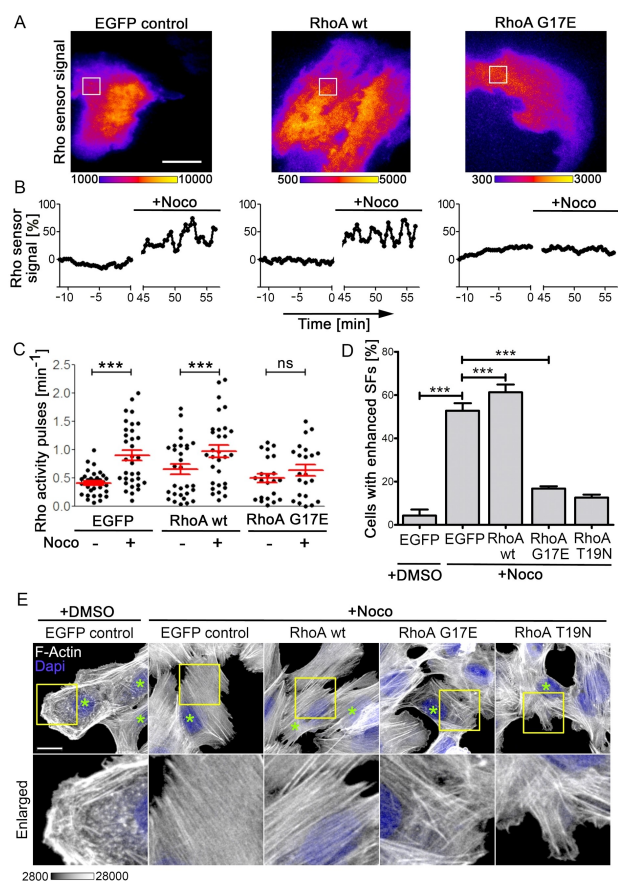

Figure 3. Dominant negative inhibition of endogenous Rho activity dynamics by Rho G17E. U2OS cells co-expressing the Rho activity sensor (mCherry-Rhotekin-GBD) and EGFP-fused RhoA wild-type or mutants were treated with nocodazole (30 μM; 45–90 min). This treatment stimulates Rho activity dynamics via the release of GEF-H1 from microtubules. EGFP alone was used as control. (A–C) TIRF-microscopy based analysis of Rho activity dynamics in U2OS cells co-expressing the indicated constructs. (A) Representative color-coded TIRF images of Rho activity in U2OS cells at t = 45 min after nocodazole addition (see also Supporting Information Movie 4). Scale bar: 20 μm. (B) Normalized Rho activity signal (% increase above initial values), measured in the white boxes in A. Time points are indicated relative to addition of nocodazole. (C) Local Rho activity pulse frequency (n = 24–34 cells from three independent experiments); ***, $P < 0.001$; paired t-test. (D–E) Modulation of stress fiber formation by RhoA mutants. Cells expressing RhoA wild-type or mutants were treated either with DMSO as vehicle control or nocodazole. After treatment, cells were fixed and co-stained with rhodamine-phalloidin and DAPI to visualize filamentous actin (F-actin; grey) and nuclei (blue). (D) Quantification of cells with enhanced stress fiber formation (see methods). (E) Confocal images of representative cells (maximum projections). Lower panels depict magnifications of boxed regions in the corresponding upper panels. Transfected cells are indicated with green asterisks. (n = 151–362 cells from three independent experiments; *, $P < 0.05$; **, $P < 0.01$; ***, $P < 0.001$; One-way ANOVA).

strong and reproducible anti-correlation between the Myosin-IIa and Rho responses additionally suggest that Myosin-IIa might inhibit Rho. It is important to note, that this analysis does not directly prove an inhibitory role for Myosin-IIa, as other components with similar response kinetics might act in parallel. Indeed, Rho and myosin are involved in many cellular processes, and highly divergent signal network topologies were proposed in various systems that include both negative and positive feedback. Our investigation focuses on the cell-

ChemBioChem

Research Article
doi.org/10.1002/cbic.202100582

Chemistry Europe
European Chemical
Societies Publishing

substrate adhesion area of U2OS cells, in which a role for myosin in mediating negative feedback regulation of Rho activity is supported by previous results,[4,6] but other systems might include different mechanisms of feedback control.[15] To investigate the particular molecular mechanisms in more detail, the presented acute perturbation-response analysis could be combined with additional manipulations, such as small molecule inhibitors, RNA interference or gene editing.

In another example, we show how molecular activity painting can directly be used to investigate complex molecular mechanisms in living cells. In particular, we measure multiple interactions of small GTPases in parallel in individual, living cells, and we used this information to derive the molecular mechanism by which the tumor-related Rho G17E mutant inhibits endogenous Rho activity and myosin contraction.

These examples demonstrate the general applicability of molecular activity painting to study dynamic signal networks, and the wide range of possibilities for its application to investigate their role in cell function and disease.

Acknowledgements

Conflict of Interest

The authors declare no conflict of interest.

[1] a) J. S. Coravos, F. M. Mason, A. C. Martin, *Trends Cell Biol.* **2017**, *27*, 276–283; b) P. Nalbant, L. Dehmelt, *Biol. Chem.* **2018**, *399*, 809–819.

[2] D. Kamps, L. Dehmelt, *ACS Chem. Biol.* **2017**, *12*, 2231–2239.

[3] X. Chen, M. Venkatachalapathy, D. Kamps, S. Weigel, R. Kumar, M. Orlich, R. Garrecht, M. Hirtz, C. M. Niemeyer, Y. W. Wu, L. Dehmelt, *Angew. Chem. Int. Ed.* **2017**, *56*, 5916–5920; *Angew. Chem.* **2017**, *129*, 6010–6014.

[4] D. Kamps, J. Koch, V. O. Juma, E. Campillo-Funollet, M. Graessl, S. Banerjee, T. Mazel, X. Chen, Y. W. Wu, S. Portet, A. Madzvamuse, P. Nalbant, L. Dehmelt, *Cell Rep.* **2020**, *33*, 108467.

[5] L. M. Costantini, M. Baloban, M. L. Markwardt, M. Rizzo, F. Guo, V. V. Verkhusha, E. L. Snapp, *Nat. Commun.* **2015**, *6*, 7670.

[6] M. Graessl, J. Koch, A. Calderon, D. Kamps, S. Banerjee, T. Mazel, N. Schulze, J. K. Jungkurth, R. Patwardhan, D. Solouk, N. Hampe, B. Hoffmann, L. Dehmelt, P. Nalbant, *J. Cell Biol.* **2017**, *216*, 4271–4285.

[7] N. Watanabe, T. J. Mitchison, *Science* **2002**, *295*, 1083–1086.

[8] K. Riento, A. J. Ridley, *Nat. Rev. Mol. Cell Biol.* **2003**, *4*, 446–456.

[9] C. S. Lee, C. K. Choi, E. Y. Shin, M. A. Schwartz, E. G. Kim, *J. Cell Biol.* **2010**, *190*, 663–674.

[10] a) M. Sakata-Yanagimoto, T. Enami, K. Yoshida, Y. Shiraishi, R. Ishii, Y. Miyake, H. Muto, N. Tsuyama, A. Sato-Otsubo, Y. Okuno, S. Sakata, Y. Kamada, R. Nakamoto-Matsubara, N. B. Tran, K. Izutsu, Y. Sato, Y. Ohta, J. Furuta, S. Shimizu, T. Komeno, Y. Sato, T. Ito, M. Noguchi, E. Noguchi, M. Sanada, K. Chiba, H. Tanaka, K. Suzukawa, T. Nanmoku, Y. Hasegawa, O. Nureki, S. Miyano, N. Nakamura, K. Takeuchi, S. Ogawa, S. Chiba, *Nat. Genet.* **2014**, *46*, 171–175; b) T. Palomero, L. Couronne, H. Khiabanian, M. Y. Kim, A. Ambesi-Impiombato, A. Perez-Garcia, Z. Carpenter, F. Abate, M. Allegretta, J. E. Haydu, X. Jiang, I. S. Lossos, C. Nicolas, M. Balbin, C. Bastard, G. Bhagat, M. A. Piris, E. Campo, O. A. Bernard, R. Rabadan, A. A. Ferrando, *Nat. Genet.* **2014**, *46*, 166–170; c) M. Kakiuchi, T. Nishizawa, H. Ueda, K. Gotoh, A. Tanaka, A. Hayashi, S. Yamamoto, K. Tatsuno, H. Katoh, Y. Watanabe, T. Ichimura, T. Ushiku, S. Funahashi, K. Tateishi, I. Wada, N. Shimizu, S. Nomura, K. Koike, Y. Seto, M. Fukayama, H. Aburatani, S. Ishikawa, *Nat. Genet.* **2014**, *46*, 583–587.

[11] T. Nishizawa, K. Nakano, A. Harada, M. Kakiuchi, S. I. Funahashi, M. Suzuki, S. Ishikawa, H. Aburatani, *Oncotarget* **2018**, *9*, 23198–23207.

[12] a) R. Khosravi-Far, P. A. Solski, G. J. Clark, M. S. Kinch, C. J. Der, *Mol. Cell. Biol.* **1995**, *15*, 6443–6453; b) S. Zhang, J. Han, M. A. Sells, J. Chernoff, U. G. Knaus, R. J. Ulevitch, G. M. Bokoch, *J. Biol. Chem.* **1995**, *270*, 23934–23936.

[13] F. Medina, A. M. Carter, O. Dada, S. Gutowski, J. Hadas, Z. Chen, P. C. Sternweis, *J. Biol. Chem.* **2013**, *288*, 11325–11333.

[14] a) M. Krendel, F. T. Zenke, G. M. Bokoch, *Nat. Cell Biol.* **2002**, *4*, 294–301; b) Y. C. Chang, P. Nalbant, J. Birkenfeld, Z. F. Chang, G. M. Bokoch, *Mol. Biol. Cell* **2008**, *19*, 2147–2153.

[15] a) A. Munjal, J. M. Philippe, E. Munro, T. Lecuit, *Nature* **2015**, *524*, 351–355; b) R. Priya, G. A. Gomez, S. Budnar, S. Verma, H. L. Cox, N. A. Hamilton, A. S. Yap, *Nat. Cell Biol.* **2015**, *17*, 1282–1293.